http://dx.doi.org/10.14500/aro.12574

Ray Tracing of Various Surface Light Trapping Structures on Silicon Solar Cells

Halo D. Omar†

Department of Physics, Faculty of Science and Health, Koya University,
Koya, Kurdistan Region – F.R. Iraq

***Abstract*—In this work, the SunSolve ray tracer is used to investigate the effects of various surface structures on silicon (Si) passivated emitter and rear cell (PERC) solar cells. A Si substrate with a thickness of 170 μm is used. The studied surface structures include front-side inverted pyramids, cones, and spherical caps. Flat Si is used as a reference. The performance of these structures is evaluated across the 200–1100 nm wavelength range under AM 1.5G solar spectrum illumination at normal incidence. The weighted-average reflectance (R_{WAR}) is calculated from the reflectance profile over the entire spectral range. Among the results, the PERC solar cell with a pyramid texture demonstrates a short-circuit current density (J_{sc}) of up to 40.55 mA/cm^2 and a conversion efficiency (η) of 21.76%. This represents a significant performance improvement over the other structures, attributed to enhanced broadband light absorbance and increased device efficiency. This study thus provides a detailed analysis of how different front-surface structures affect the performance of Si photovoltaic cells.**

***Index Terms*—Light trapping, Silicon, Solar cell, SunSolve ray tracer.**

I. Introduction

Silicon (Si) solar cells account for over 90% of the photovoltaic (PV) market due to the abundance of Si in the earth's crust, its high durability, non-toxicity, and its suitable bandgap for efficient energy conversion (Badran and Lazarov, 2025). The most dominant Si solar cell technology is based on the passivated emitter and rear cell (PERC) architecture (Blakers, 2019). To date, PERC Si solar cells hold more than 70% of the PV market share (Yan, et al., 2021). Recently, it has been reported that the average module price for PERC Si technology has reduced to about USD 0.20/Watt$_p$ (Yang, et al., 2019). For this technology, the typical thickness of a Si solar cell in industrial production is currently 170 μm (Zamchiy and Baranov, 2022).

A flat Si surface reflects more than 35% of incident sunlight at 600 nm due to its high refractive index (~3.94 at this wavelength) (Li, et al., 2012). To mitigate these reflectance losses, surface texturing is employed as a light-trapping technique to enhance light absorbance in Si solar cell. Si textures are primarily classified as either regular or random (Sreejith, et al., 2022). Studies consistently show that inverted pyramid textures outperform upright textures in PERC solar cells due to superior light trapping, leading to higher short-circuit current density (J_{sc}) and efficiency (η). In the literature, Si wafers with a thickness of about 180 μm are used to fabricate inverted and upright pyramid textures using an $AgNO_3$ (0.0001 M)/HF (4 M)/H_2O_2 (1 M) solution for 300 s, resulting in pyramid formation. As a result, the PERC solar cells with inverted pyramids demonstrated a 0.55% efficiency improvement over those with an upright pyramid texture (Gao, et al., 2021). In another study, nanocones fabricated on an ultra-thin (10 μm) Si solar cell through dry etching achieved a J_{sc} of 29 mA/cm^2 and η of 13.7%, representing a 30.6% relative improvement in J_{sc} over a flat Si solar cell. This enhancement is attributed to improved light trapping within the thin absorber (Jeong, McGehee and Cui, 2013). Using the SunSolve ray tracer, a recent study compared Si cones with and without a Si nitride (SiNx) antireflection coating (ARC). The results showed that the SiNx ARC significantly reduces reflectance. Consequently, PERC solar cells incorporating the ARC cones achieved a higher efficiency of 20.4%, compared to 20.3% for cells with uncoated cones (Pakhuruddin and Noor, 2022). In another article (McIntosh, Abbott and Sudbury, 2016), the SunSolve ray tracer was employed to analyze spherical caps at various angles (θ = 30–90°). The reflectance reached a minimum at approximately 54° across the wavelength range of 300–1100 nm. This work presents a novel study using SunSolve ray tracer simulation to analyze and compare the efficacy of various light trapping surface structures – pyramids, cones, and spherical caps – an approach not previously reported in the literature. The study identifies which structures most effectively reduce surface reflectance to enhance the optical and electrical parameters of solar cells. It reveals a strong correlation between the structures' geometric shape and both the optical performance and electrical properties.

This study employs the SunSolve simulation platform to investigate the optical and electrical performance of 170 μm-thin Si solar cells. The study focuses on the effects of various front-side surface structures – specifically pyramids,

ARO-The Scientific Journal of Koya University
Vol. XIV, No.1 (2026), Article ID: ARO.12574. 5 pages
DOI: 10.14500/aro.12574
Received: 29 August 2025; Accepted: 30 March 2026
Regular research paper; Published: 13 June 2026
†Corresponding author's e-mail: halo.dalshad@koyauniversity.org

cones, and spherical caps – on PERC device performance. To isolate the impact of texturing, no ARC is applied. Optical performance is analyzed in terms of total spectral reflectance, transmittance, and absorbance across the 200–1100 nm wavelength spectrum. Corresponding electrical parameters – including open-circuit voltage (V_{oc}), short-circuit current density (J_{sc}), fill factor (FF), efficiency (η), and current density–voltage (J-V) characteristics – are also simulated. All three light trapping structures are compared with a flat Si reference cell (untextured).

II. Methodology

In this work, the SunSolve ray tracer (by PV Lighthouse) is used to simulate the optical and electrical properties and the light-trapping effect for various surface structures on a Si PERC solar cell with 170 μm Si thickness. The optical simulations employed a standard AM 1.5G solar spectrum under an illumination of 100 mW/cm^2, a cell temperature of 25°C, and normal incidence (0° zenith angle). Here, the zenith angle is defined as the angle between the direct solar beam and the surface normal (Tahir, et al., 2024). For each wavelength in the spectral range of 200–1100 nm (at 20 nm intervals), a maximum of 50000 rays are traced. Three random surface structures – pyramids, cones, and spherical caps – are designed (Fig. 1). To generate roughness parameters, randomly distributed surface features representing the texture are created. During SunSolve ray tracing, these features influence the direction and intensity of light scattering by determining ray reflectance directions, with the random surface array further enhances scattering. A flat (planar) Si surface without texture is included as a reference. This study investigates the effect of these surface structures on the optical and electrical performance of a Si PERC solar cell, specifically without the use of ARC. The design of all surface textures aimed to maximize light absorbance by incorporating a 54.7° facet angle (optimal for Si), a randomly periodic pattern to suppress coherent scattering, and a 4 μm height to enhance the photon path length, as detailed in Table I (Pakhuruddin and Noor, 2022). The weighted average reflectance (R_{WAR}) is calculated from the measured reflectance spectrum, R(λ), using Equation (1). R_{WAR} is defined as the integral of R(λ) multiplied by the AM 1.5G spectral photon flux density, S(λ), across the 200–1100 nm spectral range (Dou, et al., 2021).

$$R_{WAR}(\lambda) = \frac{\int_{200\,nm}^{1100\,nm} R(\lambda)S(\lambda)d\lambda}{\int_{200\,nm}^{1100\,nm} R(\lambda)S(\lambda)d\lambda}$$

Silver (Ag) with a resistivity of 1.6 × 10^{-6} Ω·cm is used for front and rear contacts. The specific geometrical configurations for the fingers and busbars are based on the front contact structure of a PERC solar cell. The front side features 120 rounded rectangular finger conductors, each with a height of 15 μm and a width of 45 μm. They are spaced 0.126 cm apart on a pitch of 0.130 cm. The front also has 10 rectangular busbar conductors, each 15 μm in height and 120 μm in width. Each busbar includes 9 connection pads that are 1 μm in length and 120 μm in width.

The electrical performance parameters (V_{oc}, FF, and η) are derived by combining the optical simulation from the SunSolve with fundamental electrical theory. The J_{sc} is determined by integrating the device's absorbance profile, assuming unity carrier collection. From the J-V curve, the V_{oc} is identified as the point of zero net current, and the maximum power point (P_{max}) is located. The FF is then calculated as FF = $P_{max}/(J_{sc} \times V_{oc})$. Finally, the η is determined using the standard formula η = $(J_{sc} \times V_{oc} \times FF)/P_{in}$, where the incident power density (Pin) is set to 100 mW/cm^2 to align with standard test conditions (AM 1.5G).

III. Result and Discussion

A. Optical Characterization on Various Surface Texturing

Fig. 2 depicts the total light reflectance, transmittance, and absorbance curves for Si with various surface structures across a wavelength range of 200–100 nm. The flat Si surface demonstrates a reflectivity of roughly 35% at λ = 600 nm. Its light transmittance reaches 48% at λ = 1100 nm, which is attributable to long-wavelength light passing only once through the cell before exiting the rear (Ma Lu, et al., 2024). Overall, the flat Si exhibits weak absorbance across the measured spectrum. Textured front surfaces show improved optical performance over flat Si, featuring reduced broadband reflectance and increased absorbance. This enhancement is due to the structured front surfaces. For instance, front inverted pyramids significantly decrease reflectance across the entire wavelength region by promoting light trapping and increasing the effective absorbance path length (Huo, Fu and Peng, 2024). This structure traps incident light for multiple passes. Consequently, transmittance drops to around 10% due to the pyramid scattering effect (Pakhuruddin, et al., 2017). In contrast, front inverted cones exhibit higher reflectance than inverted pyramids across the spectrum, attributed to greater escape reflectance from the Si surface (Manzoor, et al., 2020). However, the cone texture does not significantly affect transmittance in the long-wavelength region. Front inverted spherical caps demonstrate a reflectance

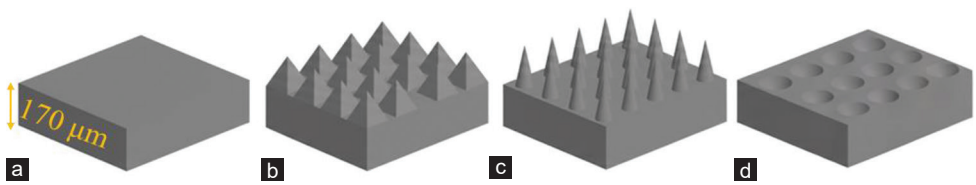

Fig. 1. Cross-sectional schematic representation of various surface structures in a silicon (Si) substrate (a) flat Si, (b) pyramids, (c) cones, and (d) spherical caps. Note that the diagrams are not to scale.

http://dx.doi.org/10.14500/aro.12574

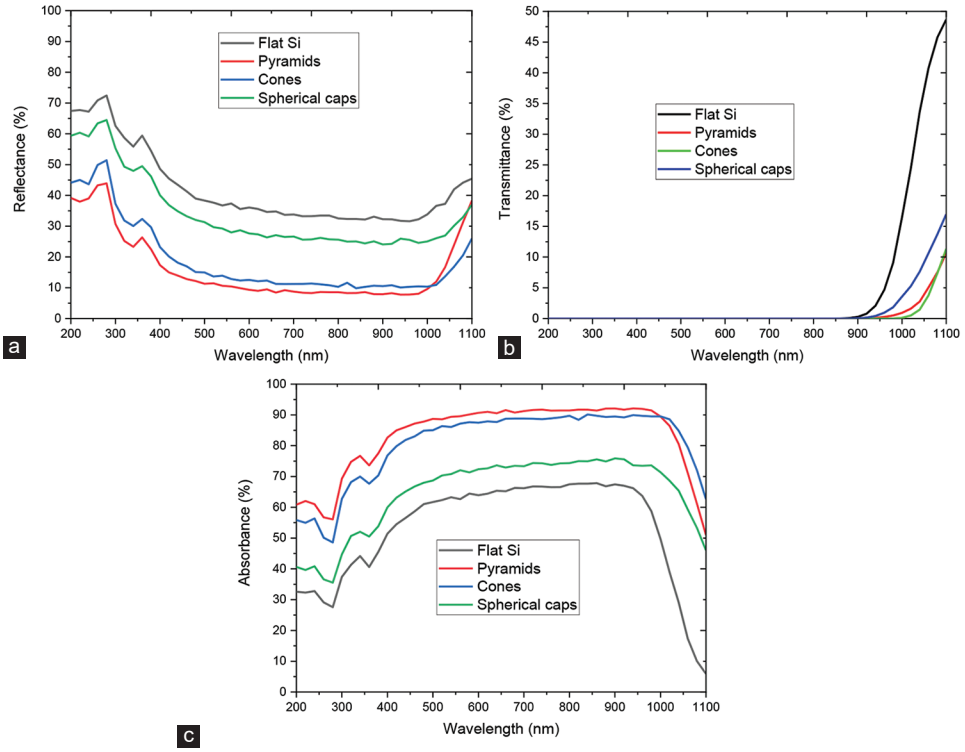

Fig. 2. (a) Total spectral reflectance, (b) light transmittance, and (c) light absorbance curves of silicon patterned with various light trapping structures: inverted pyramids, cones, and spherical caps.

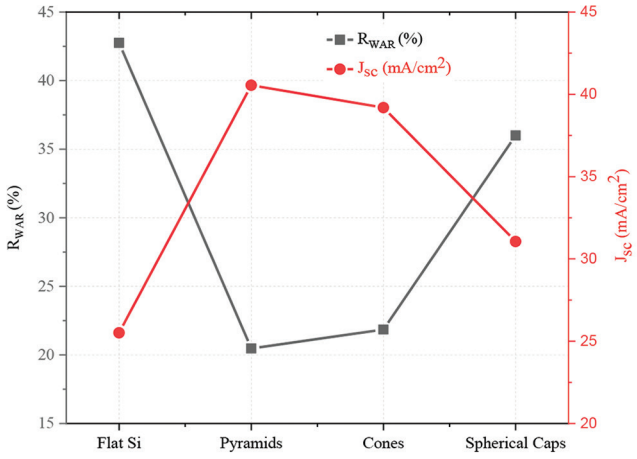

Fig. 3. R_{WAR} and potential J_{sc} for various structures on silicon (Si) surface, with flat Si shown as a reference.

of 28% and an absorbance of 72% at 600 nm. Above 900 nm, their light transmittance is slightly higher compared to inverted cones and pyramids. Comparing these textures, pyramidal structures yield the lowest front-surface reflectance. This is because pyramids scatter light more obliquely, increasing the internal path length through total internal reflection and thereby enhancing absorbance (Smith and Rohatgi, 1993; Schwartz and John, 2025). While the refractive index of Si is intrinsic and independent of surface morphology, the geometry of surface textures can create an effective graded-index effect by modifying the local angle of incidence (Wang, et al., 2022).

Fig. 3 presents the weighted average reflectance (R_{WAR}) and the corresponding short-circuit current density (J_{sc})

TABLE I
SUNSOLVE RAY TRACER SIMULATIONS UTILIZE VARIOUS STRUCTURAL PARAMETERS

Characteristics	Parameters for SunSolve ray tracer
Front textured surface: Inverted pyramids	Angle=54.7°, periodicity=random, height=4 μm, and width=5.664 μm
Front textured surface: Inverted cones	Angle=54.7°, periodicity=random, height=4 μm, and width=5.664 μm
Front textured surface: Inverted spherical caps	Angle=54.7°, periodicity=random, height=4 μm, and width=15.467 μm
Silicon thickness	170 μm
Type of Si	P-type Si
Temperature	300 (k)
Zenith incident angle	Zero (°)
Light wavelength range	200 through 1100 (nm)

Si: Silicon

TABLE II
THE INFLUENCE OF VARIOUS TEXTURE STRUCTURES ON THE ELECTRICAL PERFORMANCE OF PERC SI SOLAR CELLS

Surface texture	V_{oc} (V)	J_{sc} (mA/cm²)	FF (%)	η (%)
Flat Si	0.664	25.51	79.41	13.54
Pyramids	0.670	40.55	79.52	21.76
Cones	0.669	39.19	79.46	20.99
Spherical caps	0.667	31.06	79.43	16.57

over the wavelength range of 200–1100 nm for various surface structures on Si. Flat Si exhibits an R_{WAR} of 42.75% and a J_{sc} of 25.51 mA/cm². Light-trapping structures are commonly employed to minimize surface reflectance. The pyramidal texture reduces the R_{WAR} to 20.47%, the lowest value achieved in this work, and increases the J_{sc} to

TABLE III
ELECTRICAL PROPERTIES AND REFLECTANCE AT 600 NM FOR VARIOUS LIGHT TRAPPING DESIGNS REPORTED IN THE LITERATURE (SUNSOLVE RAY TRACING SIMULATION)

Condition	Performance	R (%) at 600 nm	J_{sc} (mA/cm^2)	V_{oc} (V)	FF (%)	η (%)	References
Flat Si	Flat Si without texture	35	25.1	0.657	79.4	13.1	(Pakhuruddin and Noor, 2022)
Flat Si	Flat Si without texture	35	26	0.658	79.4	13.6	(Rosle and Pakhuruddin, 2023)
Pyramids	Various pyramid texture angles (10–50°)	25	35	0.666	78.9	18.4	(Rosle and Pakhuruddin, 2023)
Pyramids	Different thicknesses of V_2Ox ARC (60–80 μm)/Pyramids	6	39	0.623	76	18.6	(Omar and Hamad, 2025)
Cones	SiN_X ARC/cones	10	38.6	0.669	78.7	20.3	(Pakhuruddin and Noor, 2022)
Spherical caps	Different angles (49°, 60°, 63°) of spherical caps	32.2	37.3	-	-	-	(Greulich, et al., 2015)
Pyramids	Without ARC and compared with cones and spherical caps	9	40.55	0.670	79.52	21.76	This work

ARC: Antireflection coating, FF: Fill factor, Si: Silicon

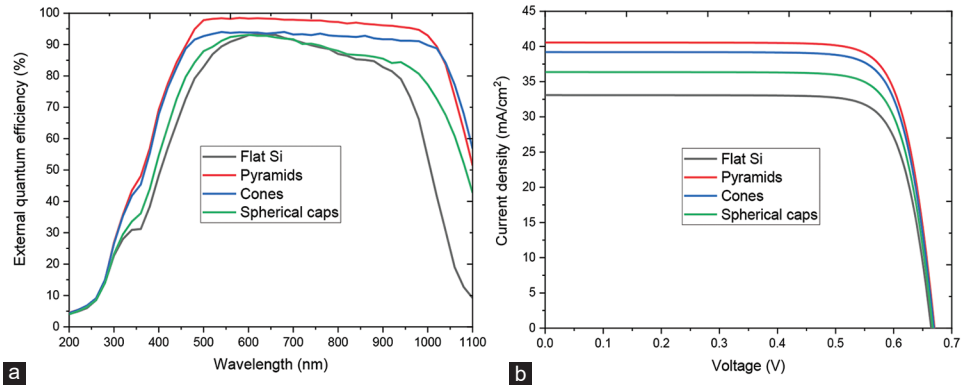

Fig. 4. (a) External quantum efficiency and (b) density–voltage profiles of the solar cell with various texture structures.

40.55 mA/cm^2. This enhancement is attributed to improved light scattering and absorbance within the Si (Omar, 2024). For the cone's structure, the J_{sc} decreases to 39.19 mA/cm^2, whereas the R_{WAR} increases to 21.85% compared to the pyramidal texture. The spherical cap structure shows a more significant reduction in performance, with a J_{sc} of 31.06 mA/cm^2 and an R_{WAR} of 36%, due to its inferior light scattering capability relative to the pyramid and cone structures.

B. Electrical Characterization on Various Surface Texturing

The external quantum efficiency (EQE), current density-voltage (J-V) characteristics, and electrical parameters of PERC Si solar cells with flat, pyramid, cone, and spherical cap surface textures are presented in Fig. 4. For the pyramid texture, the EQE spectrum of the solar cell is higher across wavelengths from 350 nm to 1100 nm compared to the cone and spherical cap surfaces. This improvement is attributed to enhanced light absorbance in the textured Si. The corresponding J-V parameters are summarized in Table II (Muhammad and Sulaiman, 2018). The flat-surface PERC solar cell exhibits the J_{sc} of 25.51 mA/cm^2 and η of 13.54%. With a cone texture, the solar cell shows a J_{sc} of 39.19 mA/cm^2, V_{oc} of 0.669 V, FF of 79.46%, and η of 20.99%. For the pyramids' texture, J_{sc} increases to 40.55 mA/cm^2 due to improved light absorbance, whereas V_{oc}, FF, and η reach 0.670 V, 79.52%, and 21.76%, respectively. The spherical cap texture yields V_{oc} = 0.667 V, J_{sc} = 31.06 mA/cm^2, FF = 79.43%, and η = 16.57%. Table III compares the electrical characteristics of solar cells with different light trapping geometries simulated using the SunSolve ray tracer, along with their surface reflectance at 600 nm, against the results of this work.

IV. CONCLUSION

This work utilizes the SunSolve ray tracer from PV lighthouse to investigate various surface structures on PERC solar cells. A 170 μm thick Si substrate is used. Three different front-surface structures are examined: inverted pyramids, cones, and spherical caps. All structures feature a random distribution with a height of 4 μm and a texture angle of 54.7°. These structures are modeled to simulate the optical and electrical properties of the PERC solar cell over the 200–1100 nm wavelength range. The AM 1.5G solar spectrum at normal incidence is used as the illumination source. A flat PERC solar cell is used as a reference in the simulation.

From the results, the flat PERC Si solar cell exhibits a J_{sc} of 25.51 mA/cm^2 and a conversion efficiency of 13.54%. The low J_{sc} is attributed to high reflectance loss from the cell's front surface. The pyramid-textured surface shows the highest broadband light absorbance, increasing the solar cell's J_{sc} and efficiency to 40.55 mA/cm^2 and 21.76%, respectively. This improvement stems from superior light scattering by the pyramids, which enhances light trapping. In contrast, the cell with cone textures shows a decrease in J_{sc} and efficiency to 39.19 mA/cm^2 and 20.99%, as its absorbance is slightly lower than that of the pyramid texture across the 200–1100 nm range. This occurs because pyramids scatter

light more obliquely, increasing the total internal reflection within Si and allowing for multiple passes that enhance absorbance. For the spherical cap texture, J_{sc} and efficiency are the lowest at 31.06 mA/cm^2 and 16.57%, due to its lower broadband absorbance compared to both pyramid and cone surfaces.

References

Badran, G., and Lazarov, V.K., 2025. From waste to resource: Exploring the current challenges and future directions of photovoltaic solar cell recycling. *Solar*, 5, p.4.

Blakers, A., 2019. Development of the PERC solar cell. *IEEE Journal of Photovoltaics*, 9, pp.629-635.

Dou, B., Jia, R., Xing, Z., Yao, X., Xiao, D., Jin, Z., and Liu, X., 2021. Enhanced performance of nanotextured silicon solar cells with excellent light-trapping properties. *Photonics*, 8, p.272.

Gao, K., Liu, Y., Cheng, H., Zhong, S., Tong, R., Kong, X., Song, X., and Huang, Z., 2021. Inverted pyramid morphology control by acid modification and application for PERC solar cells. *ACS Omega*, 6, pp.32925-32929.

Greulich, J., Volk, A.K., Wöhrle, N., Haedrich, I., Wiese, M., Hermle, M., and Rein, S., 2015. Optical Simulation and analysis of iso-textured silicon solar cells and modules including light trapping. *Energy Procedia*, 77, pp.69-74.

Huo, C., Fu, H., and Peng, K.Q., 2024. Inverted pyramid structures fabricated on monocrystalline silicon surface with a NaOH solution. *Heliyon,* 10, p.e23871.

Jeong, S., Mcgehee, M.D., and Cui, Y., 2013. All-back-contact ultra-thin silicon nanocone solar cells with 13.7% power conversion efficiency. *Nature Communications*, 4, p.2950.

Li, Y., Lee, M.Y., Cheng, H.W., and Lu, Z.L., 2012. 3D simulation of morphological effect on reflectance of Si3N4 sub-wavelength structures for silicon solar cells. *Nanoscale Research Letters*, 7, p.196.

Ma Lu, S., Amaducci, S., Gorjian, S., Haworth, M., Hägglund, C., Ma, T., Zainali, S., and Campana, P.E., 2024. Wavelength-selective solar photovoltaic systems to enhance spectral sharing of sunlight in agrivoltaics. *Joule*, 8, pp.2483-2522.

Manzoor, S., Filipič, M., Onno, A., Topič, M., and Holman, Z.C., 2020. Visualizing light trapping within textured silicon solar cells. *Journal of Applied Physics*, 127, p.063104.

Mcintosh, K.R., Abbott, M.D., and Sudbury, B.A., 2016. Ray tracing isotextured solar cells. *Energy Procedia*, 92, pp.122-129.

Muhammad, F.F., and Sulaiman, K., 2018. Thermal stability and reproducibility enhancement of organic solar cells by tris (hydroxyquinoline) gallium dopant forming a dual acceptor active layer. *ARO-The Scientific Journal of Koya University*, 6, pp.69-78.

Omar, H.D., 2024. Upright pyramid surface textures for light trapping and MoOx layer in ultrathin crystalline silicon solar cells. *Aro-The Scientific Journal of Koya University*, 12, pp.203-206.

Omar, H.D., and Hamad, S.S., 2025. Ray-tracing of vanadium oxide as anti-reflective coating on inverted pyramids silicon for solar cells. *Journal of Optics*, 54, p.1-5.

Pakhuruddin, M.Z., and Noor, N.A.M., 2022. Ray tracing of thin PERC silicon solar cells with cone textures. *Key Engineering Materials*, 930, pp.3-8.

Pakhuruddin, M.Z., Huang, J., Dore, J., and Varlamov, S., 2017. Enhanced light-trapping in laser-crystallised silicon thin-film solar cells on glass by optimised back surface reflectors. *Solar Energy*, 150, pp.477-484.

Rosle, M.A.A., and Pakhuruddin, M.Z., 2023. Investigation on absorption and photocurrent in silicon absorber with varied pyramid texture angles by ray tracer. *Key Engineering Materials*, 947, pp.47-53.

Schwartz, G., and John, S., 2025. Augmented pyramidal photonic crystals for thin silicon photovoltaics. *Optics Express*, 33, pp.16290-16304.

Smith, A.W., and Rohatgi, A., 1993. Ray tracing analysis of the inverted pyramid texturing geometry for high efficiency silicon solar cells. *Solar Energy Materials and Solar Cells*, 29, pp.37-49.

Sreejith, K.P., Sharma, A.K., Basu, P.K., and Kottantharayil, A. 2022. Etching methods for texturing industrial multi-crystalline silicon wafers: A comprehensive review. *Solar Energy Materials and Solar Cells*, 238, p.111531.

Tahir, S., Saeed, R., AshfAQ, A., Ali, A., Mehmood, K., Almousa, N., Shokralla, E.A., Macadangdang, R.R. Jr., Soeriyadi, A.H., and Bonilla, R.S., 2024. Optical modeling and characterization of bifacial SiNx/AlOx dielectric layers for surface passivation and antireflection in PERC. *Progress in Photovoltaics: Research and Applications*, 32, pp.63-72.

Wang, H.W., Yen, H., Liu, P.K., and Wang, L., 2022. Formation of inverted pyramid-like structures on surfaces of single crystalline silicon solar cells by chemical wet etching. *Journal of Renewable and Sustainable Energy*, 14, p.13501.

Yan, W.S., Tan, X.Y., Guan, L., Zhou, H.P., Yang, X.B., Xiang, P., and Zhong, Z.C., 2021. Solution of efficiency loss in thinned silicon PERC solar cells. *Renewable Energy*, 165, pp.118-124.

Yang, W., Shen, H., Jiang, Y., Tang, Q., Raza, A., and Gao, K., 2019. Formation of inverted pyramid-like submicron structures on multicrystalline silicon using nitric acid as oxidant in metal assisted chemical etching process. *Physica Status Solidi (a)*, 216, p.1800636.

Zamchiy, A.O., and Baranov, E.A., 2022. Polycrystalline silicon thin films for solar cells via metal-induced layer exchange crystallization. *Coatings*, 12, p.1926.